

1 A sub-canopy structure for simulating oil palm in the Community Land Model (CLM-Palm):
2 phenology, allocation and yield

3 Yuanchao Fan^{1,2,*}, Olivier Roupsard^{3,4}, Martial Bernoux⁵, Gueric Le Maire³, Oleg Panferov⁶,
4 Martyna M. Kotowska⁷, Alexander Knohl¹

5 ¹ University of Göttingen, Department of Bioclimatology, Büsingenweg 2, 37077 Göttingen,
6 Germany

7 ² AgroParisTech, SIBAGHE (Systèmes intégrés en Biologie, Agronomie, Géosciences,
8 Hydrosociences et Environnement), 34093 Montpellier, France

9 ³ CIRAD, UMR Eco&Sols (Ecologie Fonctionnelle & Biogéochimie des Sols et des Agro-
10 écosystèmes), 34060 Montpellier, France

11 ⁴ CATIE (Tropical Agricultural Centre for Research and Higher Education), 7170 Turrialba,
12 Costa Rica

13 ⁵ IRD, UMR Eco&Sols, 34060 Montpellier, France

14 ⁶ University of Applied Sciences Bingen, 55411 Bingen am Rhein, Germany

15 ⁷ University of Göttingen, Department of Plant Ecology and Ecosystems Research, Untere
16 Karspüle 2, 37073 Göttingen, Germany

17 *Correspondence author. E-mail: yfan1@uni-goettingen.de

18

19 **Abstract:** In order to quantify the effects of forests to oil palm conversion occurring in the
20 tropics on land-atmosphere carbon, water and energy fluxes, we develop a new perennial crop
21 sub-model CLM-Palm for simulating a palm plant functional type (PFT) within the
22 framework of the Community Land Model (CLM4.5). CLM-Palm is tested here on oil palm
23 only but is meant of generic interest for other palm crops (e.g. coconut). The oil palm has
24 monopodial morphology and sequential phenology of around 40 stacked phytomers, each
25 carrying a large leaf and a fruit bunch, forming a multilayer canopy. A sub-canopy
26 phenological and physiological parameterization is thus introduced, so that each phytomer has
27 its own prognostic leaf growth and fruit yield capacity but with shared stem and root
28 components. Phenology and carbon and nitrogen allocation operate on the different
29 phytomers in parallel but at unsynchronized steps, separated by a thermal period. An
30 important phenological phase is identified for the oil palm - the storage growth period of bud
31 and “spear” leaves which are photosynthetically inactive before expansion. Agricultural
32 practices such as transplanting, fertilization, and leaf pruning are represented. Parameters
33 introduced for the oil palm were calibrated and validated with field measurements of leaf area
34 index (LAI), yield and net primary production (NPP) from Sumatra, Indonesia. In calibration
35 with a mature oil palm plantation, the cumulative yields from 2005 to 2014 matched notably
36 well between simulation and observation (mean percentage error = 3%). Simulated inter-
37 annual dynamics of PFT-level and phytomer-level LAI were both within the range of field
38 measurements. Validation from eight independent oil palm sites shows the ability of the
39 model to adequately predict the average leaf growth and fruit yield across sites and
40 sufficiently represent the significant nitrogen and age related site-to-site variability in NPP
41 and yield. Results also indicate that seasonal dynamics of yield and remaining small-scale
42 site-to-site variability of NPP are driven by processes not yet implemented in the model or
43 reflected in the input data. The new sub-canopy structure and phenology and allocation
44 functions in CLM-Palm allow exploring the effects of tropical land use change, from natural
45 ecosystems to oil palm plantations, on carbon, water and energy cycles and regional climate.

46 **1. Introduction**

47 Land-use changes in Southeast Asia have been accelerated by economy-driven expansion of
48 oil palm (*Elaeis guineensis*) agriculture since the 1990s (Miettinen et al., 2011). Oil palm is
49 currently one of the most rapidly expanding and high-yielding crops in the world (Carrasco et
50 al., 2014) and Indonesia as the largest global palm-oil producer has planned to double its oil-
51 palm area from 9.7 million ha in 2009 to 18 million ha by 2020 (Koh and Ghazoul, 2010).
52 Since oil palms favor a tropical-humid climate with consistently high temperatures and
53 humidity, the plantations have converted large areas of rainforest in Indonesia in the past two
54 decades including those on carbon-rich peat soils (Carlson et al., 2012; Gunarso et al. 2013).
55 Undisturbed forests have long-lasting capacity to store carbon in comparison to disturbed or
56 managed vegetation (Luyssaert et al., 2008). Tropical forest to oil palm conversion has
57 significant implications on above- and belowground carbon stocks (Kotowska et al., 2015a).
58 However, the exact quantification of long-term and large-scale forest – oil palm replacement
59 effects is difficult as the greenhouse gas balance of oil palms is still uncertain due to
60 incomplete monitoring of the dynamics of oil palm plantations (including young development
61 stage), and lack of understanding of the carbon, nitrogen, water and energy exchange between
62 oil palms, soil and the atmosphere at ecosystem scale. Besides that, the assessment of these
63 processes in agricultural ecosystems is complicated by human activities e.g. crop management,
64 including planting and pruning, irrigation and fertilization, litter and residues management,
65 and yield outputs. One of the suitable tools for evaluating the feedback of oil palm expansion
66 is ecosystem modelling. Although a series of agricultural models exist for simulating the
67 growth and yield of oil palm such as OPSIM (van Kraalingen et al., 1989), ECOPALM
68 (Combres et al., 2013), APSIM-Oil Palm (Huth et al., 2014), PALMSIM (Hoffmann et al.,
69 2014), these models did not aim yet at the full picture of carbon, water and energy exchanges
70 between land and atmosphere and remain to be coupled with climate models. Given the
71 current and potential large-scale deforestation driven by the expansion of oil palm plantations,

72 the ecosystem services such as yield, carbon sequestration, microclimate, energy and water
73 balance of this new managed monoculture landscape have to be evaluated in order to estimate
74 the overall impact of land-use change on environment including regional and global climate.

75 Land surface modelling has been widely used to characterize the two-way interactions
76 between climate and human activities in terrestrial ecosystems such as deforestation,
77 agricultural expansion, and urbanization (Jin and Miller, 2011; Oleson et al., 2004). A variety
78 of land models have been adapted to simulate land-atmosphere energy and matter exchanges
79 for major crops such as the Community Land Model (CLM, Oleson et al., 2013). CLM
80 represents the crop and naturally vegetated land units as patches of plant functional types
81 (PFTs) defined by their key ecological functions (Bonan et al., 2002). However, most of the
82 crops being simulated are annual crops such as wheat, corn, soybean, etc. Their phenological
83 cycles are usually represented as three stages of development from planting to leaf emergence,
84 to fruit-fill and to harvest, all within a year. Attempts were also made to evaluate the climate
85 effects of perennial crops, e.g. by extending the growing season of annuals (Georgescu et al.,
86 2011). However the perennial crops such as oil palm, cacao, coffee, rubber, coconut, and
87 other fruiting trees and their long-term biophysical processes are not represented in the above
88 land models yet, despite the worldwide growing demand (FAO, 2013).

89 Oil palm is a perennial evergreen crop which can be described by the Corner's architectural
90 model (Hall et al., 1978). A number of phytomers, each carrying a large leaf (frond) and
91 axillating a fruit bunch, emerge successively (nearly two per month) from a single meristem
92 (the bud) at the top of a solitary stem. They form a multilayer canopy with old leaves
93 progressively being covered by new ones, until being pruned at senescence. Each phytomer
94 has its own phenological stage and yield, according to respective position in the crown. The
95 oil palm is productive for more than 25 years, including a juvenile stage of around 2 years. In
96 order to capture the inter- and intra-annual dynamics of growth and yield and land-
97 atmosphere energy, water and carbon fluxes in the oil palm system, a new structure and

98 dimension detailing the phytomer-level phenology, carbon (C) and nitrogen (N) allocation
99 and agricultural managements have to be added to the current integrated plant-level
100 physiological parameterizations in the land models. This specific refinement needs to remain
101 compliant with the current model structure though, and be simple to parameterize.

102 In this context, we develop a new CLM-Palm sub-model for simulating the growth, yield, and
103 energy and material cycling of oil palm within the framework of CLM4.5. It introduces a sub-
104 canopy phenological and physiological parameterization, so that multiple leaf and fruit
105 components operate in parallel but at delayed steps. A phytomer in the model is meant to
106 represent the average condition of an age-cohort of actual oil palm phytomers across the
107 whole plantation landscape. The overall gross primary production (GPP) by leaves and carbon
108 output by fruit harvests rely on the development trends of individual phytomers. The
109 functions implemented for oil palm combine the characteristics of both trees and crops, such
110 as the woody-like stem growth and turnover but the crop-like vegetative and reproductive
111 allocations which enable fruit C and N output. Agricultural practices such as transplanting,
112 fertilization, and leaf pruning are also represented.

113 The main objectives of this paper are to: i) describe the development of CLM-Palm including
114 its phenology, carbon and nitrogen allocation, and yield output; ii) optimize model parameters
115 using field-measured leaf area index (LAI) and observed long-term monthly yield data from a
116 mature oil palm plantation in Sumatra, Indonesia; and iii) validate the model against
117 independent LAI, yield and net primary production (NPP) data from eight oil palm
118 plantations of different age in Sumatra, Indonesia.

119 **2. Model development**

120 For adequate description of oil palm functioning, we adapted the CLM crop phenology,
121 allocation and vegetative structure subroutines to the monopodial morphology and sequential
122 phenology of oil palm so that each phytomer evolves independently in growth and yield (Fig.

123 1). Their phenology sequence is determined by the phyllochron (the period in thermal time
124 between initiations of two subsequent phytomers) (Table A1). A maximum of 40 phytomers
125 with expanded leaves, each growing up to 7-m long, are usually maintained in plantations by
126 pruning management. There are also around 60 initiated phytomers developing slowly inside
127 the bud. The largest ones, already emerged at the top of the crown but unexpanded yet, are
128 named “spear” leaves (Fig. 1a). Each phytomer can be considered a sub-PFT component that
129 has its own prognostic leaf growth and fruit yield capacity but having 1) the stem and root
130 components that are shared by all phytomers, 2) the soil water content, nitrogen resources,
131 and resulting photosynthetic assimilates that are also shared and partitioned among all
132 phytomers, and 3) a vertical structure of the foliage, with the youngest at the top and the
133 oldest at the bottom of the canopy. Within a phytomer the fruit and leaf components do not
134 compete for growth allocation because leaf growth usually finishes well before fruit-fill starts.
135 However one phytomer could impact the other ones through competition for assimilates,
136 which is controlled by the C and N allocation subroutine according to their respective
137 phenological stages.

138 Here we describe only the new phenology, allocation and agricultural management functions
139 developed for the oil palm. Photosynthesis, respiration, water and nitrogen cycles and other
140 biophysical processes already implemented in CLM4.5 (Oleson et al., 2013) are not modified
141 (except N retranslocation scheme) for the current study. The following diagram shows the
142 new functions and their coupling with existing modules within the CLM4.5 framework (Fig.
143 2).

144 **2.1. Phenology**

145 Establishment of the oil palm plantation is implemented with two options: seed sowing or
146 transplanting of seedlings. In this study, the transplanting option is used. We design 7 post-
147 planting phenological steps for the development of each phytomer: 1) leaf initiation; 2) start
148 of leaf expansion; 3) leaf maturity; 4) start of fruit-fill; 5) fruit maturity and harvest; 6) start of

149 leaf senescence; and 7) end of leaf senescence and pruning (Fig. 1b). The first two steps
150 differentiate pre-expansion (heterotrophic) and post-expansion (autotrophic) leaf growth
151 phases. The other steps control leaf and fruit developments independently so that leaf growth
152 and maturity could be finished well before fruit-fill and leaf senescence could happen after
153 fruit harvest according to field observations. The modified phenology subroutine controls the
154 life cycle of each phytomer (sub-PFT level) as well as the planting, stem and root turnover,
155 vegetative maturity (start of fruiting) and final rotation (replanting) of the whole plant (PFT
156 level). Detailed description of oil palm phenology and nitrogen retranslocation during
157 senescence is in the Supplementary materials. The main phenological parameters are in Table
158 A1.

159 All phytomers are assumed to follow the same phenological steps, where the thermal length
160 for each phase is measured by growing degree-days (GDD; White et al., 1997). For oil palm,
161 a new GDD variable with 15 °C base temperature and 25 degree-days daily maximum (Corley
162 and Tinker, 2003; Goh, 2000; Hormaza et al., 2012) is accumulated from planting (abbr.
163 GDD₁₅). The phenological phases are signaled by respective GDD requirements, except that
164 pruning is controlled by the maximum number of expanded phytomers according to
165 plantation management (Table A1). Other processes in the model such as carbon and nitrogen
166 allocation for growth of new tissues respond to this phenology scheme at both PFT level and
167 phytomer level.

168 **2.2. Carbon and Nitrogen allocation**

169 In CLM, the fate of newly assimilated carbon from photosynthesis is determined by a coupled
170 C and N allocation routine. Potential allocation for new growth of various plant tissues is
171 calculated based on allocation coefficients and their allometric relationship (Table A2).

172 A two-step allocation scheme is designed for the sub-canopy phytomer structure and
173 according to the new phenology. First, available C (after subtracting respiration costs) is

174 partitioned to the root, stem, overall leaf, and overall fruit pools with respect to their relative
 175 demands by dynamic allocation functions according to PFT-level phenology. The C:N ratios
 176 for different tissues link C demand and N demand so that a N down-regulation mechanism is
 177 enabled to rescale GPP and C allocation if N availability from soil mineral N pool and
 178 retranslocated N pool does not meet the demand. Then, the actual C and N allocated to the
 179 overall leaf or fruit pools are partitioned between different phytomers at the sub-PFT level
 180 (Fig. 2). Details are described below.

181 2.2.1. PFT level allocation

182 C and N allocation at the PFT level is treated distinctly before and after oil palm reaches
 183 vegetative maturity. At the juvenile stage before fruiting starts (i.e. $GDD_{15} < GDD_{min}$) all the
 184 allocation goes to the vegetative components. The following equations are used to calculate
 185 the allometric ratios for partitioning available C and N to the leaf, stem, and root pools.

$$186 \quad A_{root} = a_{root}^i - (a_{root}^i - a_{root}^f) \frac{DPP}{Age_{max}}, \quad (\text{Eq. 1})$$

$$187 \quad A_{leaf} = f_{leaf}^i \times (1 - A_{root}) \quad (\text{Eq. 2})$$

$$188 \quad A_{stem} = 1 - A_{root} - A_{leaf} \quad (\text{Eq. 3})$$

189 where $\frac{DPP}{Age_{max}} \leq 1$, DPP is the days past planting, and Age_{max} is the maximum plantation age
 190 (~25 years). a_{root}^i and a_{root}^f are the initial and final allocation coefficients for roots and f_{leaf}^i
 191 is the initial leaf allocation coefficient before fruiting (Table A2). Root and stem allocation
 192 ratios are calculated with Eqs. 1 and 3 for all ages and phenological stages of oil palm.

193 After fruiting begins, the new non-linear function is used for leaf allocation:

$$194 \quad A_{leaf} = a_{leaf}^2 - (a_{leaf}^2 - a_{leaf}^f) \left(\frac{DPP - DPP_2}{Age_{max} \times d_{mat} - DPP_2} \right)^{d_{alloc}^{leaf}} \quad (\text{Eq. 4})$$

195 where a_{leaf}^2 equals the last value of A_{leaf} calculated right before fruit-fill starts and DPP_2 is
 196 the days past planting right before fruit-fill starts. d_{mat} controls the age when the leaf
 197 allocation ratio approaches its final value a_{leaf}^f , while d_{alloc}^{leaf} determines the shape of change
 198 (convex when $d_{alloc}^{leaf} < 1$; concave when $d_{alloc}^{leaf} > 1$). A_{leaf} stabilizes at a_{leaf}^f when $DPP \geq$
 199 $Age_{max}d_{mat}$. The equations reflect changed vegetative allocation strategy that shifts
 200 resources to leaf for maintaining LAI and increasing photosynthetic productivity when
 201 fruiting starts. The three vegetative allocation ratios A_{leaf} , A_{stem} and A_{root} always sum to 1.

202 At the reproductive phase a fruit allocation ratio A_{fruit} is introduced, which is relative to the
 203 total vegetative allocation unity. To represent the dynamics of reproductive allocation effort
 204 of oil palm, we adapt the stem allocation scheme for woody PFTs in CLM, in which
 205 increasing NPP results in increased allocation ratio for the stem wood (Oleson et al., 2013). A
 206 similar formula is used for reproductive allocation of oil palm so that it increases with
 207 increasing NPP:

$$208 \quad A_{fruit} = \frac{2}{1+e^{-b(NPP_{mon}-100)}} - a \quad (\text{Eq. 5})$$

209 where NPP_{mon} is the monthly sum of NPP from the previous month calculated with a run-
 210 time accumulator in the model. The number 100 ($\text{g C m}^{-2} \text{ mon}^{-1}$) is the base monthly NPP
 211 when the palm starts to yield (Kotowska et al., 2015a). Parameters a and b adjust the base
 212 allocation rate and the slope of change, respectively (Table A2). This function generates a
 213 dynamic curve of A_{fruit} increasing from the beginning of fruiting to full vegetative maturity,
 214 which is used in the allocation allometry to partition assimilates between vegetative and
 215 reproductive pools (Fig. 3).

216 2.2.2. Sub-PFT (phytomer) level allocation

217 Total leaf and fruit allocations are partitioned to the different phytomers according to their
 218 phenological stages. Fruit allocation per phytomer is calculated with a sink size index:

$$219 \quad S_p^{fruit} = \frac{GDD_{15} - H_p^{F.fill}}{H_p^{F.mat} - H_p^{F.fill}}, \quad (\text{Eq. 6})$$

220 where p stands for the phytomer number, $H_p^{F.fill}$ and $H_p^{F.mat}$ are the phenological indices for
 221 the start of fruit-fill and fruit maturity (with $H_p^{F.fill} \leq GDD_{15} \leq H_p^{F.mat}$). S_p^{fruit} increases
 222 from zero at the beginning of fruit-fill to the maximum of 1 right before harvest for each
 223 phytomer. This is because the oil palm fruit accumulates assimilates at increasing rate during
 224 development until the peak when it becomes ripe and oil synthesis dominates the demand
 225 (Corley and Tinker, 2003). The sum of S_p^{fruit} for all phytomers gives the total reproductive

226 sink size index. Each phytomer receives a portion of fruit allocation by $\frac{S_p^{fruit}}{\sum_{p=1}^n S_p^{fruit}} \times A_{fruit}$,

227 where A_{fruit} is the overall fruit allocation by Eq. 5.

228 An important allocation strategy for leaf is the division of displayed versus storage pools for
 229 the pre-expansion and post-expansion leaf growth phases. These two types of leaf C and N
 230 pools are distinct in that only the displayed pools contribute to LAI growth, whereas the
 231 storage pools support the growth of unexpanded phytomers, i.e. bud & spear leaves, which
 232 remain photosynthetically inactive. Total C and N allocation to the overall leaf pool is divided
 233 to the displayed and storage pools by a fraction lf_{disp} (Table A2) according to the following
 234 equation:

$$235 \quad \begin{aligned} A_{leaf}^{display} &= lf_{disp} \times A_{leaf} \\ A_{leaf}^{storage} &= (1 - lf_{disp}) \times A_{leaf} \end{aligned} \quad (\text{Eq. 7})$$

236 The plant level $A_{leaf}^{display}$ and $A_{leaf}^{storage}$ are then distributed evenly to expanded and
 237 unexpanded phytomers, respectively, at each time step. When a phytomer enters the leaf

238 expansion phase, C and N from its leaf storage pools transfer gradually to the displayed pools
239 during the expansion period. Therefore, a transfer flux is added to the real-time allocation flux
240 and they together contribute to the post-expansion leaf growth.

241 LAI is calculated only for each expanded phytomer according to a constant specific leaf area
242 (SLA) and prognostic amount of leaf C accumulated by phytomer n . In case it reaches the
243 prescribed maximum ($PLAI_{max}$), partitioning of leaf C and N allocation to this phytomer
244 becomes zero.

245 **2.3. Other parameterizations**

246 Nitrogen retranslocation is performed exclusively during leaf senescence and stem turnover.
247 A part of N from senescent leaves and from the portion of live stem that turns dead is
248 remobilized to a separate N pool that feeds plant growth or reproductive demand. Nitrogen of
249 fine roots is all moved to the litter pool during root turnover. We do not consider N
250 retranslocation from live leaves, stem and roots specifically during grain-fill that is designed
251 for annual crops (Drewniak et al., 2013) because oil palm has continuous fruit-fill year around
252 at different phytomers.

253 The fertilization scheme for oil palm is adapted to the plantation management generally
254 carried out in our study area, which applies fertilizer biannually, starting only 6 years after
255 planting, assuming each fertilization event lasts one day. Currently the CLM-CN
256 belowground routine uses an unrealistically high denitrification rate under conditions of
257 nitrogen saturation, e.g. after fertilization, which results in a 50% loss of any excess soil
258 mineral nitrogen per day (Oleson et al., 2013). This caused the simple biannual regular
259 fertilization nearly useless because peak N demand by oil palm is hard to predict given its
260 continuous fruiting and vegetative growth and most fertilized N is thus lost in several days.
261 The high denitrification factor has been recognized as an artifact (Drewniak et al., 2013; Tang
262 et al., 2013). According to a study on a banana plantation in the tropics (Veldkamp and Keller,

263 1997), around 8.5% of fertilized N is lost as nitrogen oxide (N_2O and NO). Accounting
264 additionally for a larger amount of denitrification loss to gaseous N_2 , we modified the daily
265 denitrification rate from 0.5 to 0.001, which gives a 30% annual loss of N due to
266 denitrification that matches global observations (Galloway et al., 2004).

267 The irrigation option is turned off because oil palm plantations in the study area are usually
268 not irrigated. Other input parameters for oil palm such as its optical, morphological, and
269 physiological characteristics are summarized in Table A3. Most of them are generalized over
270 the life of oil palm.

271 **3. Model evaluation**

272 **3.1. Site data**

273 Two oil palm plantations in the Jambi province of Sumatra, Indonesia provide data for
274 calibration. One is a mature industrial plantation at PTPN-VI (01 °41.6' S, 103 °23.5' E, 2186
275 ha) planted in 2002, which provides long-term monthly harvest data (2005 to 2014). Another
276 is a 2-year young plantation at a nearby smallholder site Pompa Air (01 °50.1' S, 103 °17.7' E,
277 5.7 ha). The leaf area and dry weight at multiple growth stages were measured by sampling
278 leaflets of phytomers at different ranks (+1 to +20) on a palm and repeating for 3 different
279 ages within the two plantations. The input parameter SLA (Table A2) was derived from leaf
280 area and dry weight (excluding the heavy rachis). The phytomer-level LAI was estimated
281 based on the number of leaflets (90-300) per leaf of a certain rank and the PFT-level LAI was
282 estimated by the number of expanded leaves (35-45) per palm of a certain age. In both cases,
283 a planting density of 156 palms per hectare (8m × 8m per palm) was used according to
284 observation.

285 Additionally, LAI, yield and NPP measurements from eight independent smallholder oil palm
286 plantations (50m × 50m each) were used for model validation. Four of these sites (HO1, HO2,
287 HO3, HO4, 11-18 years old) are located in the Harapan region nearby PTPN-VI, and another

288 four (BO2, BO3, BO4, BO5, 10-14 years old) are in Bukit Duabelas region (02°04' S, 102°
289 47' E), both in Jambi, Sumatra. Fresh bunch harvest data were collected at these sites for a
290 whole year in 2014. Harvest records from both PTPN-VI and the 8 validation sites were
291 converted to harvested carbon (g C/m^2) with mean wet/dry weight ratio of 58.65 % and C
292 content 60.13 % per dry weight according to C:N analysis (Kotowska et al., 2015a). The oil
293 palm monthly NPP and its partitioning between fruit, leaf, stem and root were estimated
294 based on measurements of fruit yield (monthly), pruned leaves (monthly), stem increment
295 (every 6 month) and fine root samples (once in a interval of 6-8 month) at the eight validation
296 sites (Kotowska et al., 2015b).

297 The amount of fertilization at the industrial plantation PTPN-VI was $456 \text{ kg N ha}^{-1} \text{ yr}^{-1}$,
298 applied regularly twice per year since 6-year old. The smallholder plantations in Harapan (H
299 plots) and Bukit Duabelas (B plots) used much less fertilizer. From interview data, the H plots
300 had roughly regular N fertilization (twice per year), whereas among the B plots only BO3
301 indicated one fertilization event per year but the amount was unclear (applied chicken manure
302 in 2013) and the other plots had no N fertilization in 2013 and 2014 due to financial difficulty.
303 Fertilization history prior to 2013 is unavailable for all the smallholder plantations. Given the
304 limited information, we consider two levels of fertilization for H plots (regular: 96 kg N ha^{-1}
305 yr^{-1} , from 6-year old until 2014) and B plots (reduced: $24 \text{ kg N ha}^{-1} \text{ yr}^{-1}$, from 6-year old until
306 2012), respectively.

307 The mean annual rainfall (the Worldclim database: <http://www.worldclim.org> (Hijmans et al.,
308 2005); average of 50 years) of the two investigated landscapes in Jambi Province was ~ 2567
309 mm y^{-1} in the Harapan region (including PTPN-VI) and $\sim 2902 \text{ mm y}^{-1}$ in the Bukit Duabelas
310 region. In both areas, May to September represented a markedly drier season (30% less
311 precipitation) in comparison to the rainy season between October and April. Air temperature
312 is relatively constant throughout the year with an annual average of $26.7 \text{ }^\circ\text{C}$. In both
313 landscapes, the principal soil types are Acrisols: in the Harapan landscape loam Acrisols

314 dominate, whereas in Bukit Duabelas the majority is clay Acrisol. Soil texture such as
315 sand/silt/clay ratios and soil organic matter C content were measured at multiply soil layers
316 (down to 2.5m) (Allen et al., 2015). They were used to create two sets of surface input data
317 for the two regions separately.

318 **3.2. Model setup**

319 The model modifications and parameterizations were implemented according to CLM4.5
320 standards. A new sub-PFT dimension called *phytomer* was added to all the new variables so
321 that the model can output history tapes of their values for each phytomer and prepare restart
322 files for model stop and restart with bit-for-bit continuity. Simulations were set up in point
323 mode (a single 0.5×0.5 degree grid) at every 30-min time step. A spin-up procedure (Koven et
324 al., 2013) was followed to get a steady-state estimate of soil C and N pools, with the CLM-
325 CN decomposition cascade and broadleaf evergreen tropical forest PFT. The soil C and N
326 pools were rescaled to match the average field observation at two reference lowland rainforest
327 sites in Harapan and Bukit Duabelas regions (Allen et al., 2015; Guillaume et al., 2015),
328 which serve as the initial conditions. The forest was replaced with the oil palm at a specific
329 year of plantation establishment (2002 for PTPN-VI and 1996, 1997, 1999, 2000, 2001, 2002,
330 2003, 2004 for HO3, HO1, HO2, BO2, BO3, BO4, HO4, BO5, respectively). The oil palm
331 functions were then turned on and simulations continued until 2014. The 3-hourly ERA
332 Interim climate data (Dee et al., 2011) were used as atmospheric forcing.

333 **3.3. Calibration of key parameters**

334 A simulation from 2002 to 2014 at the PTPN-VI site was used for model calibration. Both the
335 PFT level and phytomer level LAI development were calibrated with field observations in
336 2014 from a chronosequence approach (space for time substitution) using oil palm samples of
337 three different age and multiple phytomers of different rank (section 3.1). Simulated yield
338 outputs (around twice per month) were calibrated with monthly harvest records of PTPN-VI

339 plantation from 2005 to 2014. Cumulative yields were compared because the timing of
340 harvest in the plantations was largely uncertain and varied depending on weather and other
341 conditions.

342 To simplify model calibration, we focused on parameters related to the new phenology and
343 allocation processes. Phenological parameters listed in Table A1 were determined according
344 to field observations and existing knowledge about oil palm growth phenology (Combres et
345 al., 2013; Corley and Tinker, 2003) as well as plantation management in Sumatra, Indonesia.
346 Allocation coefficients in Table A2 were more uncertain and they were the key parameters to
347 optimize in order to match observed LAI and yield dynamics according to the following
348 sensitivity analysis. Measurements of oil palm NPP and its partitioning between fruit, canopy,
349 stem, and root from the eight sites (section 3.1) were used as a general reference when
350 calibrating the allocation coefficients.

351 Leaf C:N ratio and *SLA* were determined by field measurements. Other C:N ratios and optical
352 and morphological parameters in Table A3 were either fixed by field observations or adjusted
353 in-between trees and crops.

354 **3.4. Sensitivity analysis**

355 Performing a full sensitivity analysis of all parameters used in simulating oil palm (more than
356 100 parameters, though a majority are shared with natural vegetation and other crops) would
357 be a challenging work. As with calibration, we limited the sensitivity analysis to a set of
358 parameters introduced for the specific PFT and model structure designed for oil palm (Tables
359 A1 and A2). Among the phenological parameters, *mxlivenp* (maximum number of expanded
360 phytomers) and *phyllochron* (Table A1) are closely related to pruning frequency but they
361 should not vary widely for a given oil palm breed and plantation condition. Therefore, they
362 were fixed at the average level for the study sites in Jambi, Sumatra. Parameter $PLAI_{max}$ is
363 only meant for error controlling, although in our simulations phytomer-level LAI never

364 reached $PLAI_{max}$ (see Fig. 5 in results) because environmental constraints and nitrogen down-
365 regulation already limited phytomer leaf growth well within the range. GDD_{mit} was kept to
366 zero because only the transplanting scenario was considered for seedling establishment.

367 We tested two hypotheses of phytomer level leaf development based on the other
368 phenological parameters: 1) considering the leaf storage growth period, that is, the bud &
369 spear leaf phase is explicitly simulated with the GDD parameters in Table A1 and $lf_{disp} = 0.3$
370 in Table A2; 2) excluding the storage growth period by setting $GDD_{exp} = 0$ and $lf_{disp} = 1$ so
371 that leaf expands immediately after initiation and leaf C and N allocation all goes to the
372 photosynthetic active pools.

373 The sensitivity of allocation and photosynthesis parameters in Table A2 were tested by adding
374 or subtracting 10% or 30% to the baseline values (calibrated) one-by-one and calculating their
375 effect on final cumulative yield at the end of simulation (December 2014). In fact, all the
376 allocation parameters are interconnected because they co-determine photosynthesis capacity
377 and respiration costs as partitioning to the different vegetative and reproductive components
378 varies. This simple approach provides a starting point to identify sensitive parameters,
379 although a more sophisticated sensitivity analysis is needed in the future.

380 **3.5. Validation**

381 In this study, we only validated the model structure and model behavior on simulating
382 aboveground C dynamics and partitioning as represented by LAI, fruit yield and NPP.
383 Independent leaf measurement, yield and monthly NPP data collected in 2014 from the eight
384 mature oil palm sites (H and B plots) were compared with the eight simulations using the
385 same model settings and calibrated parameters, except that two categories of climate forcing,
386 surface input data (for soil texture) and fertilization (regular vs. reduced) were prescribed for
387 the H plots and B plots, respectively.

388 4. Results

389 4.1. Calibration with LAI and yield

390 In calibration with the industrial PTPN-VI plantation, the PFT-level LAI dynamics simulated
391 by the model incorporating the pre-expansion phase matches well with the LAI measurements
392 for three different ages (Fig. 4). Simulated LAI for the PFT increases with age in a sigmoid
393 relationship. The dynamics of LAI is also impacted by pruning and harvest events because oil
394 palms invest around half of their assimilates into fruit yield. Oil palms are routinely pruned by
395 farmers to maintain the maximum number of expanded leaves around 40. Hence, when yield
396 begins 2-3 years after planting, LAI recurrently shows an immediate drop after pruning and
397 then quickly recovers. The pruning frequency decreases with age because the phyllochron
398 increases to 1.5 times at 10-year old (Supplementary materials). Simulations without the pre-
399 expansion storage growth phase show an unrealistic fast increase of LAI before 3 years old,
400 much higher than observed in the field. At older age after yield begins, LAI drops drastically
401 and recovers afterwards. Although the final LAI could stabilize at a similar level, the initial
402 jump and drop of LAI at young stage do not match field observations and cannot be solved by
403 adjusting parameters other than GDD_{exp} . Hereafter, all simulations were run using the pre-
404 expansion phase.

405 The phytomer level LAI development is comparable with leaf samples from the field (Fig. 5).
406 The two leaf samples at rank 5 (LAI = 0.085) and rank 20 (LAI = 0.122) of a mature oil palm
407 in PTPN-VI (the two black triangles for 2014) are within the range of simulated values. The
408 other sample at rank 25 (LAI = 0.04, for 2004) of a young oil palm in Pompa Air (smallholder
409 plantation) is lower than the simulated value. Each horizontal color bar clearly marks the
410 post-expansion leaf phenology cycle, including gradual increment of photosynthetic LAI
411 during phytomer development and gradual declining during senescence. The pre-expansion
412 phase is not included in the figure but model outputs show that roughly 60-70% of leaf C in a
413 phytomer is accumulated before leaf expansion, which is co-determined by the allocation

414 ratio lf_{disp} and the lengths of two growth phases set by GDD_{exp} and $GDD_{L.mat}$. This is
415 comparable to observations on coconut palm that dry mass of the oldest unexpanded leaf
416 accounts for 60% of that of a mature leaf (Navarro et al., 2008). Only when the palm becomes
417 mature, phytomer LAI could come closer to the prescribed $PLAI_{max}$ (0.165). However, during
418 the whole growth period from 2002 to 2014 none of the phytomers have reached $PLAI_{max}$,
419 which is the prognostic result of the carbon balance simulated by the model.

420 The cumulative yield of baseline simulation has overall high consistency with harvest records
421 (Fig. 6). The mean percentage error (MPE) is only 3%. The slope of simulated curve
422 increases slightly after 2008 when the LAI continues to increase and NPP reaches a high level
423 (Fig. 3). The harvest records also show the same pattern after 2008 when heavy fertilization
424 began ($456 \text{ kg N ha}^{-1} \text{ yr}^{-1}$).

425 The per-month harvest records exhibit strong zig-zag pattern (Fig. 7). One reason is that oil
426 palms are harvested every 15-20 days and summarizing harvest events by calendar month
427 would result in uneven harvest times per month, e.g. two harvests fall in a previous month and
428 only one in the next month. Yet it still shows that harvests at PTPN-VI plantation dominated
429 from October to December whereas in the earlier months of each year harvest amounts were
430 significantly lower. The simulated monthly yield has less seasonal fluctuation, but it responds
431 to the fluctuation of precipitation (Fig. 7). A slight positive linear correlation exists between
432 simulated yield and the mean precipitation of a 60-day period (corresponds to the main fruit-
433 filling and oil synthesis period) before each harvest event (Pearson's $r = 0.15$). Examining the
434 longer term year-to-year variability, a clear increasing trend of yield with increasing
435 plantation age is captured by the model, largely matching field records since the plantation
436 began to yield in 2005.

437 **4.2. Sensitivity analysis**

438 The leaf nitrogen fraction in Rubisco (F_{LNR}) is shown to be the most sensitive parameter (Fig.
 439 8), because it determines the maximum rate of carboxylation at 25 °C (V_{cmax25}) together with
 440 SLA (also sensitive), foliage nitrogen concentration (CN_{leaf} , Table A3) and other constants.
 441 Given the fact that F_{LNR} should not vary widely in nature for a specific plant, we constrained
 442 this parameter within narrow boundaries to get a V_{cmax25} around 100.7, the same as that shared
 443 by all other crop PFTs in CLM. We fixed SLA to 0.013 by field measurements. The value is
 444 only representative of the photosynthetic leaflets. The initial root allocation ratio (a_{root}^i) has
 445 considerable influence on yield because it modifies the overall respiration cost along the
 446 gradual declining trend of fine root growth across 25 years (Eq. 1). The final ratio (a_{root}^f) has
 447 limited effects because its baseline value (0.1) is set very low and thus the percentage changes
 448 are insignificant. The leaf allocation coefficients (f_{leaf}^i , a_{leaf}^f) are very sensitive parameters
 449 because they determine the magnitudes of LAI and GPP and consequently yield. The
 450 coefficients d_{mat} and d_{alloc}^{leaf} control the nonlinear curve of leaf development (Eq. 4) and
 451 hence the dynamics of NPP and that partitioned to fruits. Increased F_{stem}^{live} results in higher
 452 proportion of live stem throughout life, given the fixed stem turnover rate (Supplementary
 453 materials), and therefore it brings higher respiration cost and lower yield. The relative
 454 influence of fruit allocation coefficients a and b on yield is much lower than the leaf
 455 allocation coefficients because of the restriction of A_{fruit} by NPP dynamics (Eq. 5).
 456 Parameters lf_{disp} and $transplant$ have negligible effects. lf_{disp} has to work together with the
 457 phenological parameter GDD_{exp} to give a reasonable size of spear leaves before expansion
 458 according to field observation. The sensitivity of GDD_{exp} is shown in Fig. 4. Varying the size
 459 of seedlings at transplanting by 10% or 30% does not alter the final yield, likely because the
 460 initial LAI is still within a limited range (0.1~0.2) given the baseline value 0.15.

461 **4.3. Model validation with independent dataset**

462 The LAI development curves for the eight oil palm sites follow similar patterns since field
 463 transplanting in different years, except that the B plots (BO2, BO3, BO4) are restrained in

464 LAI growth after 11 years old because of reduced fertilization (Fig. 9a). The field data in
465 2014 also shows the check by N limitation and even exhibits a decreasing trend of LAI with
466 increasing plantation age at B plots except BO5 which is under 10 years old (Fig. 9b). In
467 general, the modelled LAI has a positive relationship with plantation age under regularly
468 fertilized condition and it stabilizes after 15-year old (site HO3) as controlled by d_{mat} (Eq. 4).
469 This age-dependent trend is observed in the field with a notable deviation by site HO1. The
470 average LAI of the eight sites from the model is comparable with field measurement in 2014
471 (MPE = 13%). There are large uncertainties in field LAI estimates because we did not
472 measure LAI at the plot level directly but only sampled leaf area and dry weight of individual
473 phytomers and scaled the values up.

474 The simulated annual yields match closely with field observations in 2014 at both the H plots
475 (MPE = 2%) and B plots (MPE = 2%; Fig. 10). With regular fertilization in the H plots, both
476 the modelled and observed yield are slightly higher in the older plantations (HO2, HO1, and
477 HO3) than the younger one (H04) but stabilize around $1280 \text{ g C m}^{-2} \text{ yr}^{-1}$ past the age of 15
478 years. In contrast, the B plots have significantly lower yield because of reduced N input and
479 the model is able to capture the N limitation effect on both NPP and yield, i.e. the declining
480 trend with increasing age, which is consistent with field observation. The model simulates
481 slightly higher NPP than field estimates at 7 smallholder sites (MPE = 10%) using the input
482 parameters calibrated and optimized only for LAI and yield at the industrial PTPN-VI
483 plantation. Field measured leaf NPP only includes leaf litter production but does not account
484 for the growing size of canopy (i.e. increasing LAI).

485 **5. Discussion**

486 Calibration and validation with multiple site data demonstrate the utility of CLM-Palm and its
487 sub-canopy structure for simulating the growth and yield of the unique oil palm plantation
488 system within a land surface modeling context.

489 The pre-expansion phenological phase is proved necessary for simulating both phytomer-
490 level and PFT-level LAI development in a prognostic manner. The leaf C storage pool
491 provides an efficient buffer to support phytomer development and maintain overall LAI
492 during fruiting. It also avoids an abnormally fast increase of LAI in the juvenile stage when C
493 and N allocation is dedicated to the vegetative components. Without the leaf storage pool, the
494 plant's canopy develops unrealistically fast at young age and then enters an emergent drop
495 once fruit-fill begins (Fig. 4). This is because the plant becomes unable to sustain leaf growth
496 just from its current photosynthetic assimilates when a large portion is allocated to fruits.

497 The model well simulates year-to-year variability in yield (Fig. 7), in which the increasing
498 trend is closely related to the fruit allocation function (Fig. 3) and LAI development (Fig. 4).
499 The seasonal variability in simulated yield corresponds to the precipitation data but it is
500 difficult to interpret the difference with monthly harvest records due to the artificial zig-zag
501 pattern. The harvest records from plantations do not necessarily correspond to the amount of
502 mature fruits along a phenological time scale due to varying harvest arrangements, e.g. fruits
503 are not necessarily harvested when they are ideal for harvest, but when it is convenient.
504 Observations of mature fruits on a tree basis (e.g. Navarro et al., 2008 on coconut) would be
505 more suitable to compare with modeled yield, but such data are not available at our sites.
506 Some studies have also demonstrated important physiological mechanisms on oil palm yield
507 including inflorescence gender determination and abortion rates that both respond to seasonal
508 climatic dynamics although with a time lag (Combres et al., 2013; Legros et al., 2009). The
509 lack of representation of such physiological traits might affect the seasonal dynamics of yield
510 simulated by our model, but these mechanisms are rarely considered in a land surface
511 modelling context. Nevertheless, the results correspond generally to the purpose of our
512 modelling which is focused on the long-term climatological effects of oil palm agriculture.
513 The correct representation of multi-year trend of carbon balance which we did reach is more
514 important than the correct prediction of each yield. For latter the more agriculturally-oriented
515 models should be used.

516 Resource allocation patterns for perennial crops are more difficult to simulate than annual
517 crops. For annuals, the LAI is often assumed to decline during grain-fill (Levis et al., 2012).
518 However, the oil palm has to sustain a rather stable leaf area while partitioning a significant
519 amount of C to the fruits. The balance between reproductive and vegetative allocations is
520 crucial. The dynamics of A_{fruit} as a function of monthly NPP is proved useful to capture the
521 increasing yield capacity of oil palms during maturing at favorable conditions (Fig. 6, 7) and
522 also able to adjust fruit allocation and shift resources to the vegetative components under
523 stress conditions (e.g. N limitation, Fig. 9 and 10). The value of A_{fruit} increased from 0.5 to
524 1.5 (Fig. 3), resulting more than a half partitioning of NPP to the reproductive pool at mature
525 stage which matched closely with field observations (Fig. 10; Kotowska et al., 2015a;
526 Kotowska et al., 2015b). Our experiments (not shown here) confirmed that the dynamic
527 function is more robust than a simple time-dependent or vegetation-size-dependent allocation
528 function.

529 The phenology and allocation processes in land surface models are usually aimed to represent
530 the average growth trend of a PFT at large spatial scale (Bonan et al., 2002; Drewniak et al.,
531 2013). We made a step forward by comparing point simulations with multiple specific site
532 observations. The model predicts well the average LAI development and yield as well as NPP
533 of mature plantations across two different regions. Site-to-site variability in yield and NPP at
534 the Harapan and Bukit Duabelas plots under contrasting conditions (regular vs. reduced
535 fertilization) is largely captured by the model. The decreasing trend of yield and pause of LAI
536 growth in B plots after 10 years old (Fig. 9, 10) reflect reduced N availability observed in the
537 clay Acrisol soil in Bukit Duabelas (Allen et al., 2015) with very limited C and N return from
538 leaf litter because of pruning and piling of highly lignified leaves (Guillaume et al., 2015).
539 Yet there remains small-scale discrepancy in LAI, NPP or yield in some sites which is
540 possibly due to the fact that microclimate, surface input data and the amount and timing of
541 fertilization were only prescribed as two categories for H and P plots, respectively. Field data
542 show the proportion of NPP allocated to yield is significantly higher in plot HO1 (70%) than

543 in other plots (50% to 65%) which could explain the low LAI of HO1. This is not reflected in
544 the model as the same parameters are used in the fruit allocation function (Eq. 5) across sites.
545 The deviation in allocation pattern is likely due to difference in plantation management (e.g.
546 harvest and pruning cycles), which has been shown to be crucial for determining vegetative
547 and reproductive growth (Euler et al., 2015). Other factors such as insects, fungal infection,
548 and possibly different oil palm progenies could also result in difference in oil palm growth
549 and productivity, but they are typically omitted in land surface models. Generalized input
550 parameterization across a region is usually the case when modeling with a PFT, although a
551 more complex management (e.g. dynamic fertilization) scheme could be devised and
552 evaluated thoroughly with additional field data, which we lack at the moment.

553 Overall, the sub-canopy phytomer-based structure, the extended phenological phases for a
554 perennial crop PFT and the two-step allocation scheme of CLM-Palm are distinct from
555 existing functions in land surface models. The phytomer configuration is similar to the one
556 already implemented in other oil palm growth and yield models such as the APSIM-Oil Palm
557 model (Huth et al., 2014) or the ECOPALM yield prediction model (Combres et al., 2013).
558 But the implementation of this sub-canopy structure is the first attempt among land surface
559 models. CLM-Palm incorporates the ability of an agricultural model for simulating growth
560 and yield, beside that it allows the modeling of biophysical and biogeochemical processes as a
561 land model should do, e.g. what is the whole fate of carbon in plant, soil and atmosphere if
562 land surface composition shifts from a natural system to the managed oil palm system? In a
563 following study, a fuller picture of the carbon, nitrogen, water and energy fluxes over the oil
564 palm landscape are examined with CLM-Palm presented here and evaluated with Eddy
565 Covariance flux observation data. We develop this palm sub-model in the CLM framework as
566 it allows coupling with climate models so that the feedbacks of oil palm expansion to climate
567 can be simulated in future steps.

568 **6. Conclusions**

569 The development of CLM-Palm including canopy structure, phenology, and carbon and
570 nitrogen allocation functions was proposed for modeling an important agricultural system in
571 the tropics. This paper demonstrates the ability of the new palm module to simulate the inter-
572 annual dynamics of vegetative growth and fruit yield from field planting to full maturity of
573 the plantation. The sub-canopy-scale phenology and allocation strategy are necessary for this
574 perennial evergreen crop which yields continuously on multiple phytomers. The pre-
575 expansion leaf storage growth phase is proved essential for buffering and balancing overall
576 vegetative and reproductive growth. Average LAI, yield and NPP are satisfactorily simulated
577 for multiple sites, which fulfills the main mission of a land surface modeling approach, that is,
578 to represent the average conditions and dynamics of large-scale processes. On the other hand,
579 simulating small-scale site-to-site variation (50m × 50m sites) requires detailed input data on
580 site conditions (e.g. microclimate) and plantation managements that are often not available
581 thus limiting the applicability of the model at small scale. Nevertheless, the CLM-Palm model
582 sufficiently represents the significant region-wide variability in oil palm NPP and yield driven
583 by nutrient input and plantation age in Jambi, Sumatra. The point simulations here provide a
584 starting point for calibration and validation at large scales.

585 To be run in a regional or global grid, the age class structure of plantations needs to be taken
586 into account. This can be achieved by setting multiple replicates of the PFT for oil palm, each
587 planted at a point of time at a certain grid. As a result, a series of oil palm cohorts developing
588 at different grids could be configured with a transient PFT distribution dataset, which allows
589 for a quantitative analysis of the effects of land-use changes, specifically rainforest to oil palm
590 conversion, on carbon, water and energy fluxes. This will contribute to the land surface
591 modeling community for simulating this structurally unique, economically and ecologically
592 sensitive, and fast expanding oil palm land cover.

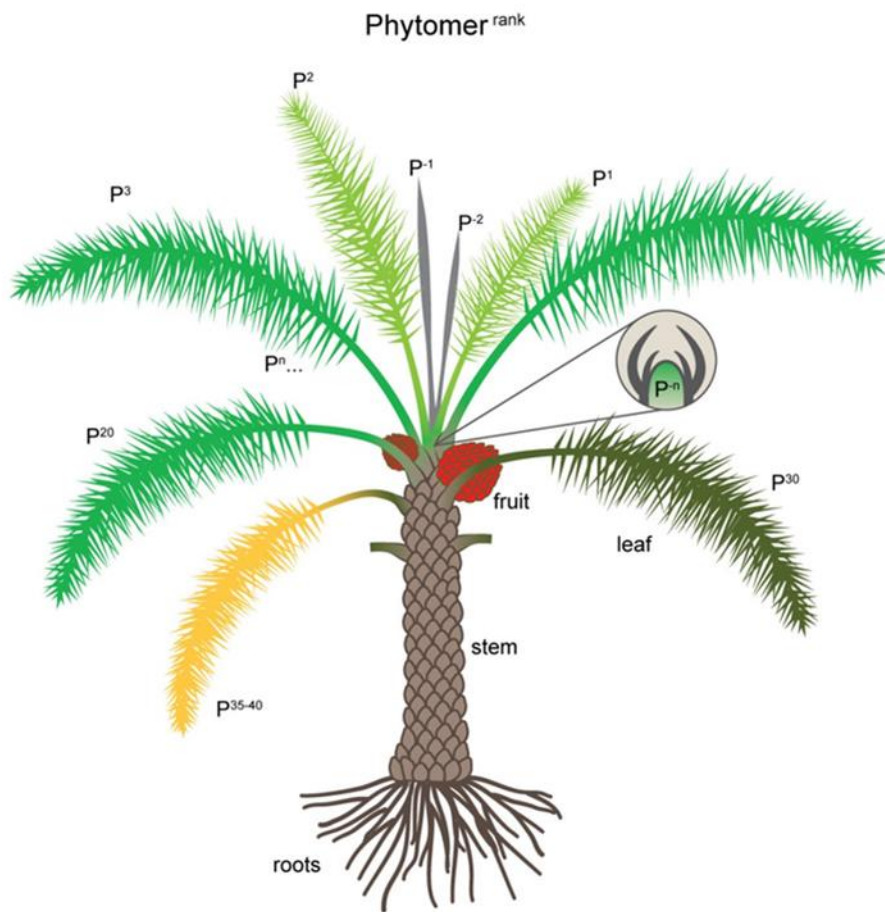
593 **Acknowledgements:**

594 This study was funded by the European Commission Erasmus Mundus FONASO Doctorate
595 fellowship. Field trips were partly supported by the Collaborative Research Centre 990

596 (Ecological and Socioeconomic Functions of Tropical Lowland Rainforest Transformation
597 Systems (Sumatra, Indonesia)) funded by the German Research Foundation (DFG). We are
598 grateful to Kara Allen (University of Göttingen, Germany), Dr. Bambang Irawan (University
599 of Jambi, Indonesia) and the PTPN-VI plantation in Jambi for providing field data on oil palm.
600 The source code of the post-4.5 version CLM model was provided by Dr. Samuel Levis from
601 National Center for Atmospheric Research (NCAR), Boulder, CO, USA.

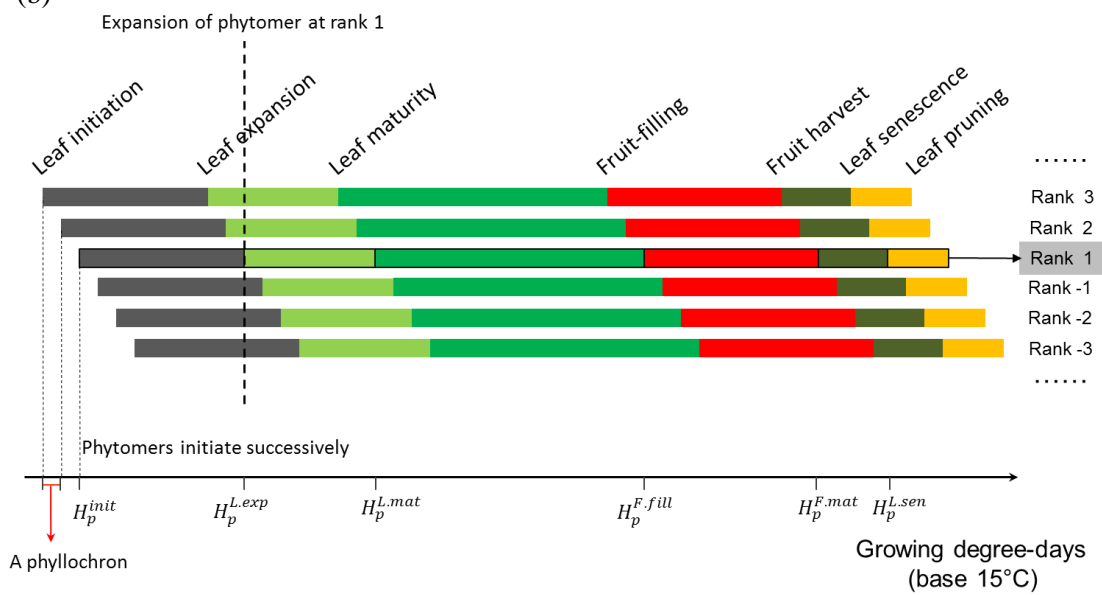
602 This open-access publication was funded by the University of Göttingen.

(a)



604

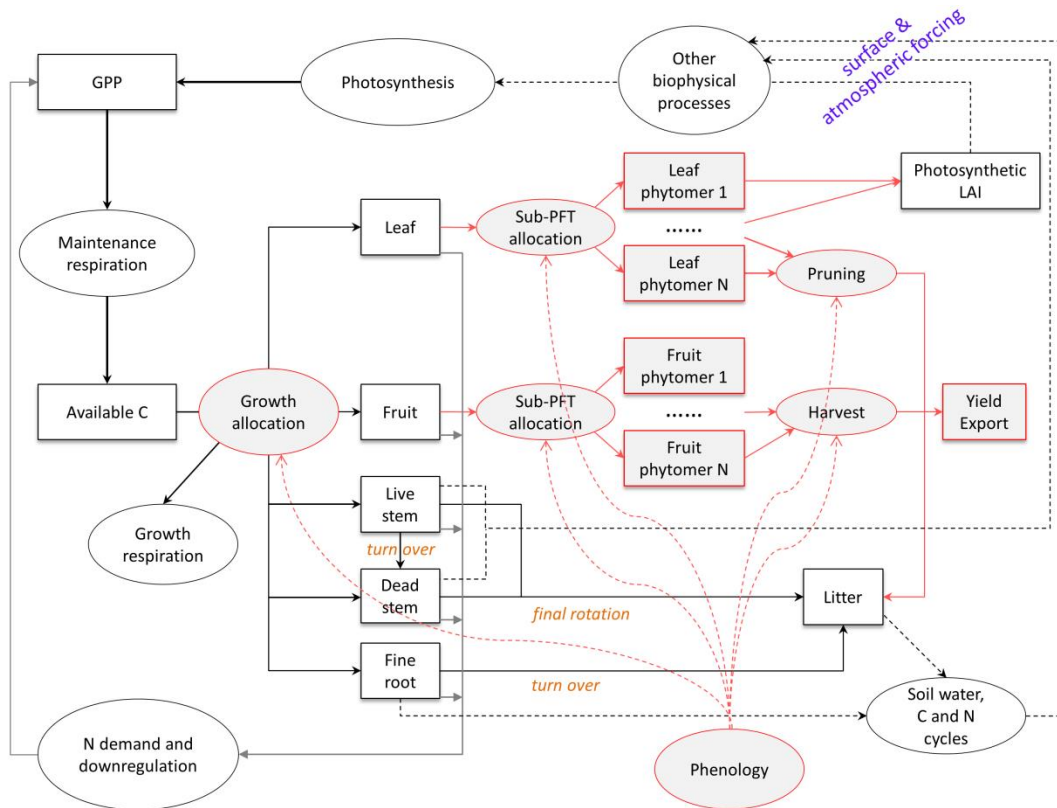
(b)



605

606 Fig. 1. (a) New sub-canopy phytomer structure of CLM-Palm. P^1 to P^n indicate expanded
 607 phytomers and P^{-1} to P^{-n} at the top indicate unexpanded phytomers packed in the bud. Each
 608 phytomer has its own phenology, represented by different colors corresponding to: (b) the
 609 phytomer phenology: from initiation to leaf expansion, to leaf maturity, to fruit-fill, to harvest,
 610 to senescence and to pruning. Phytomers initiate successively according to the phyllochron
 611 (the period in heat unit between initiations of two subsequent phytomers). Detailed phenology
 612 description is in Supplementary materials.

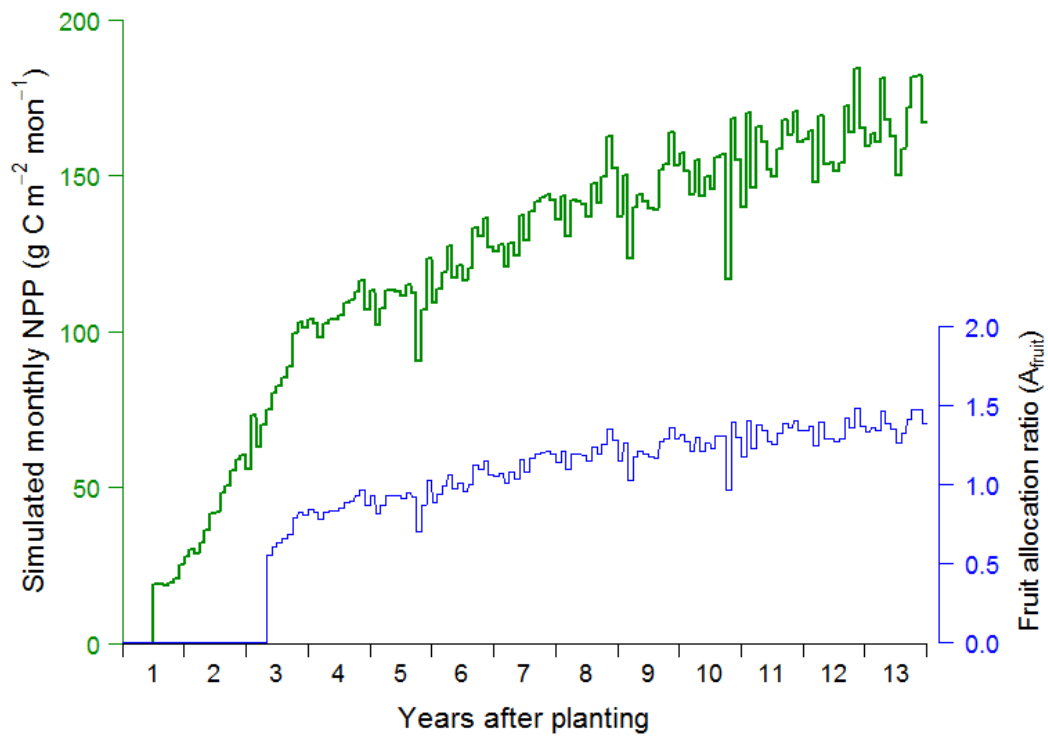
613



614

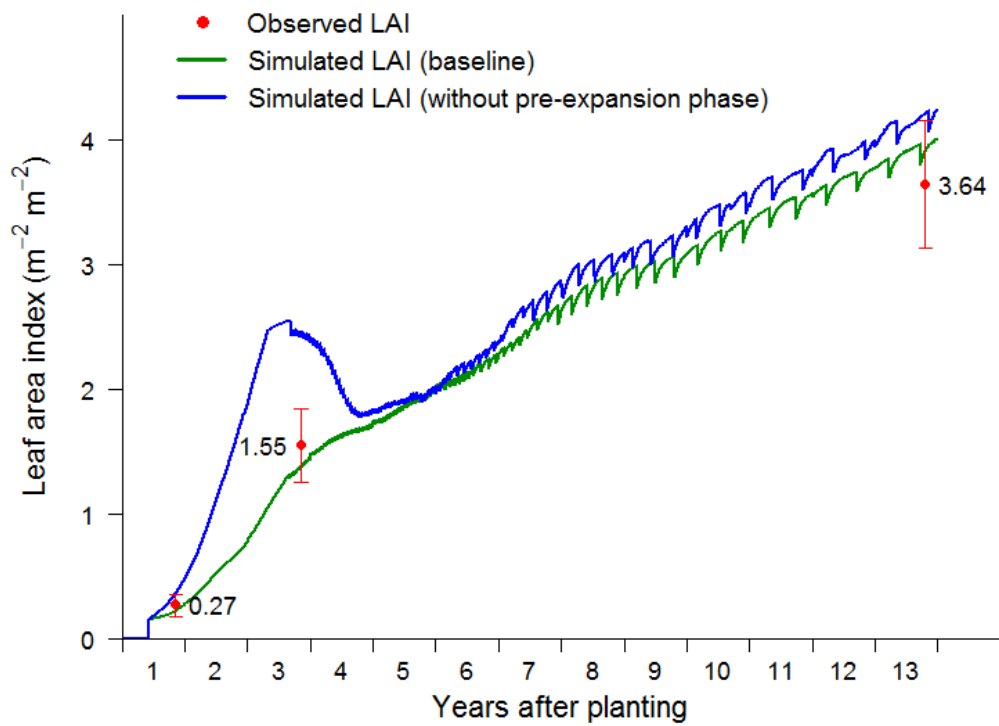
615 Fig. 2. Original and modified structure and functions for developing CLM-Palm in the
 616 framework of CLM4.5. Original functions from CLM4.5 are represented in black or grey.
 617 New functions designed for CLM-Palm are represented in red, including phenology,
 618 allocation, pruning, fruit harvest and export, as well as the sub-canopy (sub-PFT) structure.

619



620

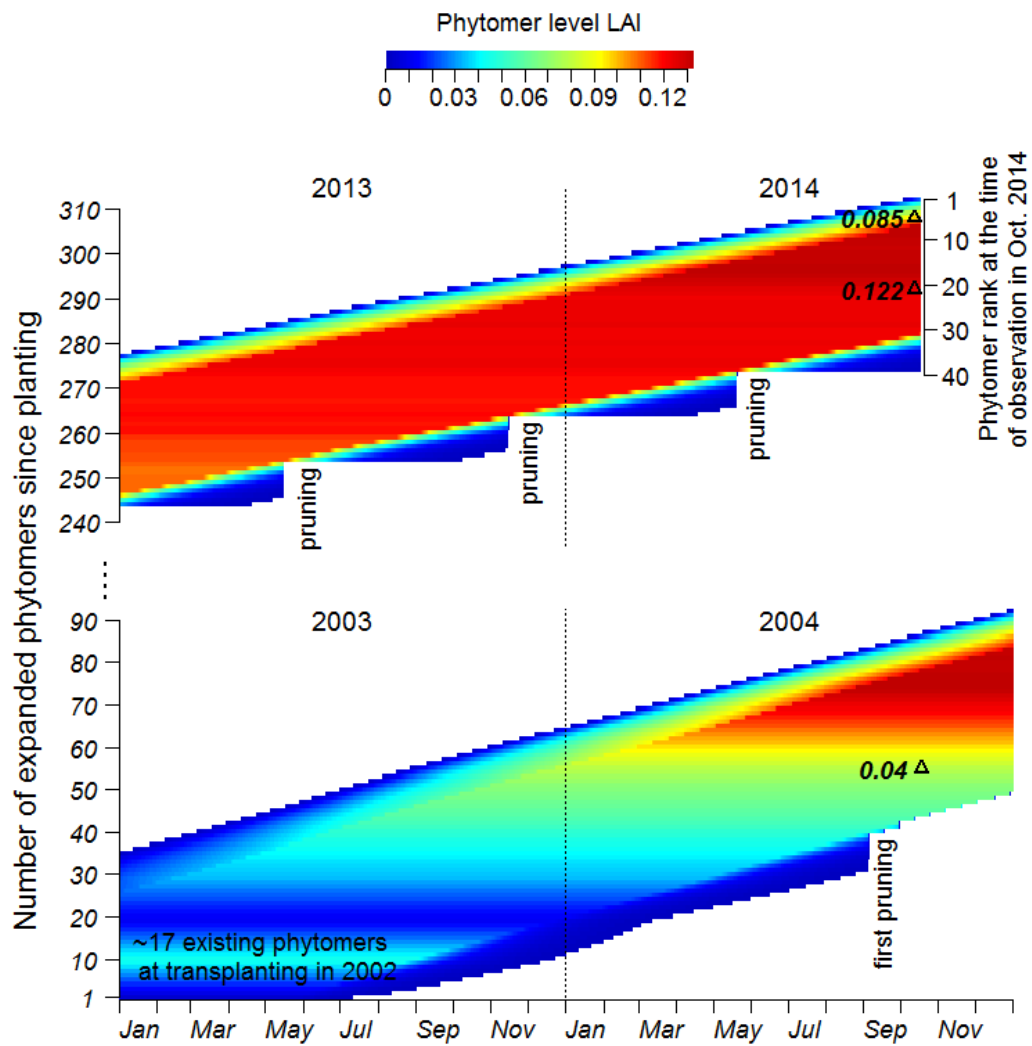
621 Fig. 3. Time course of reproductive allocation rate (blue line) in relation to monthly NPP from
 622 the previous month (NPP_{mon} , green line) according to Eq. 5. A_{fruit} is relative to the vegetative
 623 unity ($A_{leaf} + A_{stem} + A_{root} = 1$ and $0 \leq A_{fruit} \leq 2$). The NPP_{mon} was simulated with
 624 calibrated parameters for the PTPN-VI site.



625

626 Fig. 4. PFT-level LAI simulated by CLM-Palm, with and without the pre-expansion growth
 627 phase in the phytomer phenology and compared to field measurements used for calibration.
 628 The initial sudden increase at year 1 represents transplanting from nursery. The sharp drops
 629 mark pruning events.

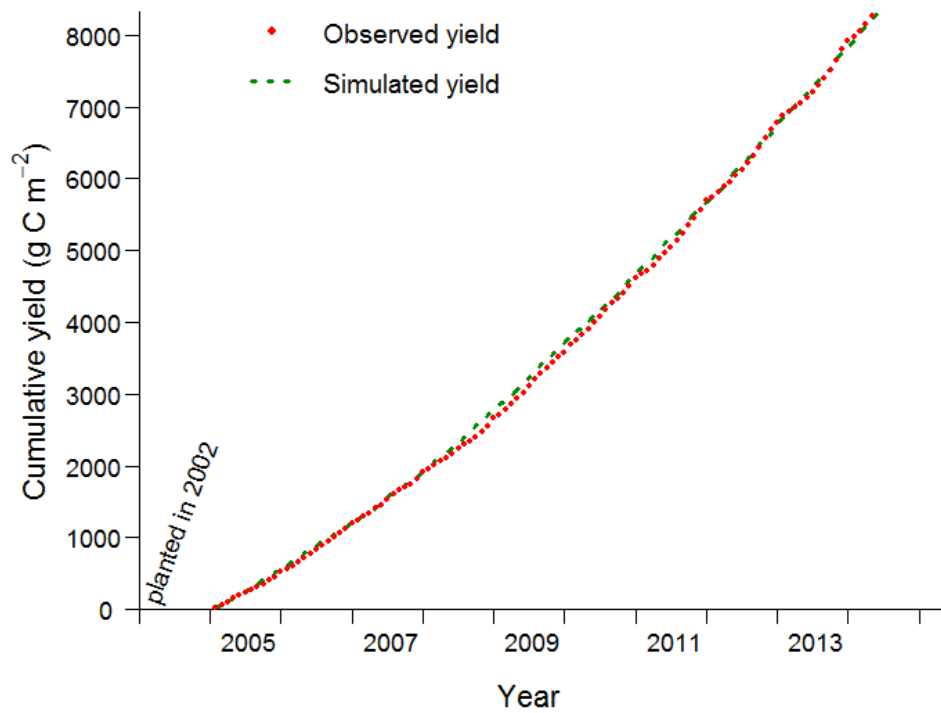
630



631

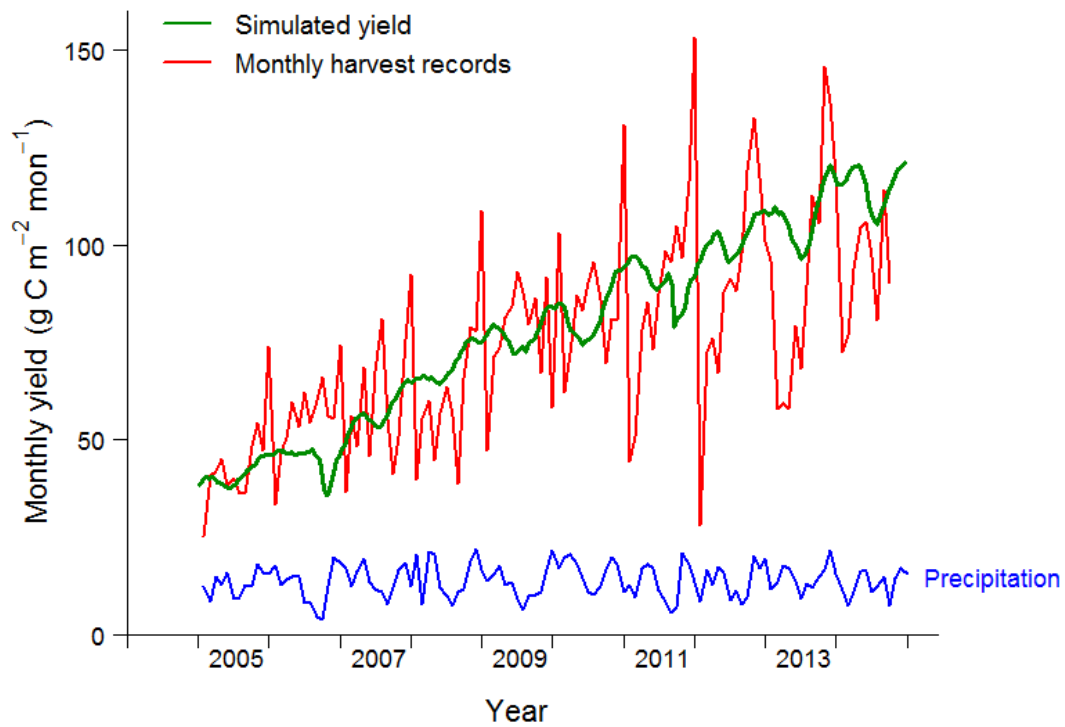
632 Fig. 5. Simulated phytomer level LAI dynamics (horizontal color bar) compared with field
 633 observations (black triangles with measured LAI value). The newly expanded phytomer at a
 634 given point of time has a rank of 1. Each horizontal bar represents the life cycle of a phytomer
 635 after leaf expansion. Phytomers emerge in sequence and the y-axis gives the total number of
 636 phytomers that have expanded since transplanting in the field. Senescent phytomers are
 637 pruned.

638



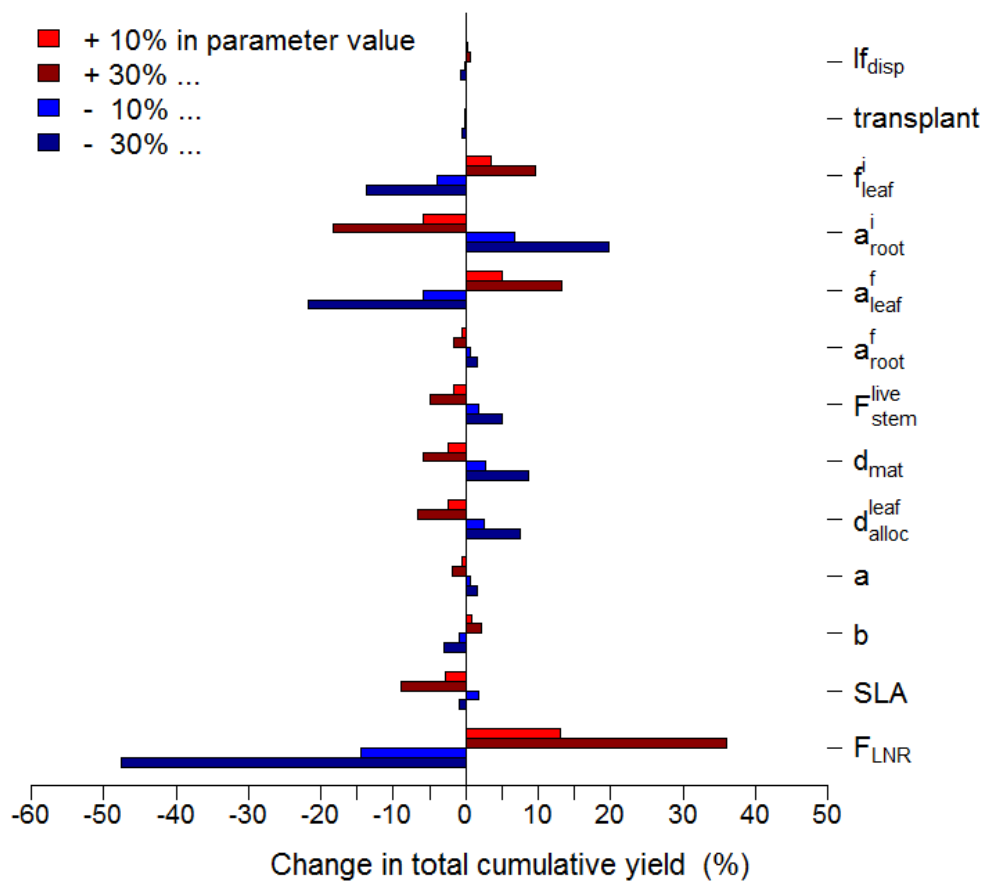
639

640 Fig. 6. Simulated PFT-level yield compared with monthly harvest data (2005-2014) from the
 641 calibration site PTPN-VI in Jambi, Sumatra. CLM-Palm represents multiple harvests from
 642 different phytomers (about twice per month). The cumulative harvest amounts throughout
 643 time are compared.



644

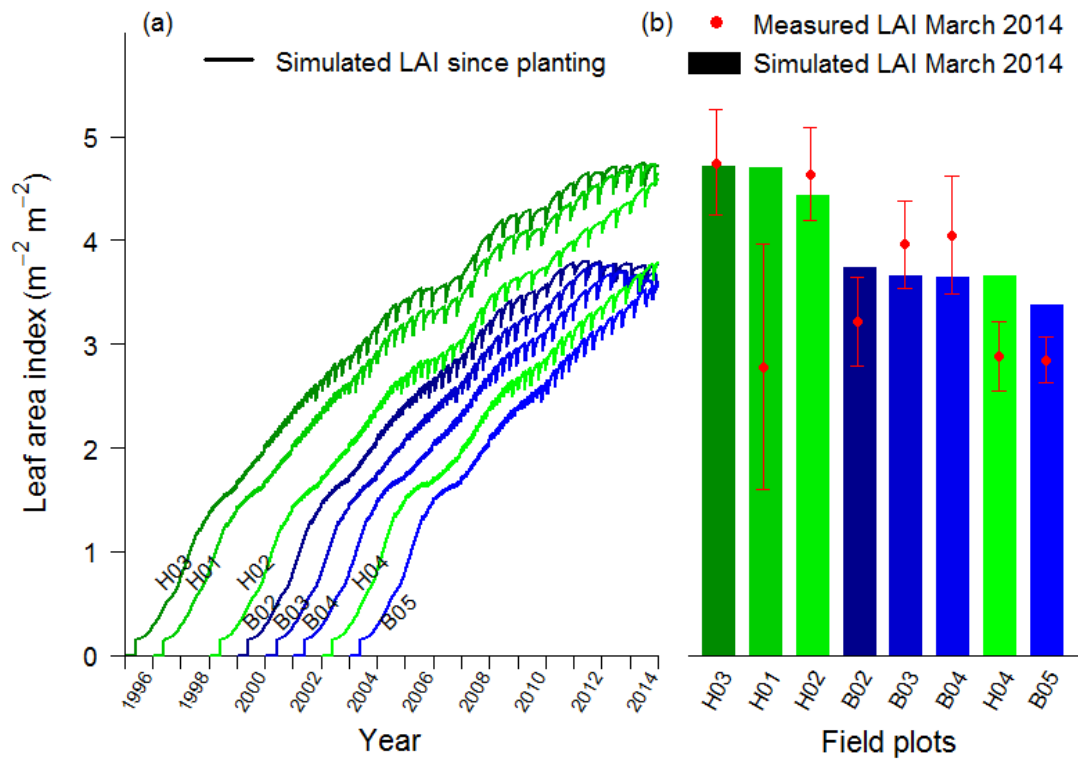
645 Fig. 7. Simulated and observed monthly yield at PTPN-VI compared with monthly
 646 precipitation dynamics (mean: 206 mm per month). The modeled yield outputs are per harvest
 647 event (every 15-20 days depending on the phyllochron), while harvest records are the
 648 summary of harvest events per month. The model output is thus rescaled to show the monthly
 649 trend of yield that matches the mean of harvest records, given that the cumulative yields are
 650 almost the same between simulation and observation as shown in Fig. 6.



651

652 Fig. 8. Sensitivity analysis of key allocation parameters in regard of the cumulative yield at
 653 the end of simulation, with two magnitudes of change in the value of a parameter one-by-one
 654 while others are hold at the baseline values in Table A2.

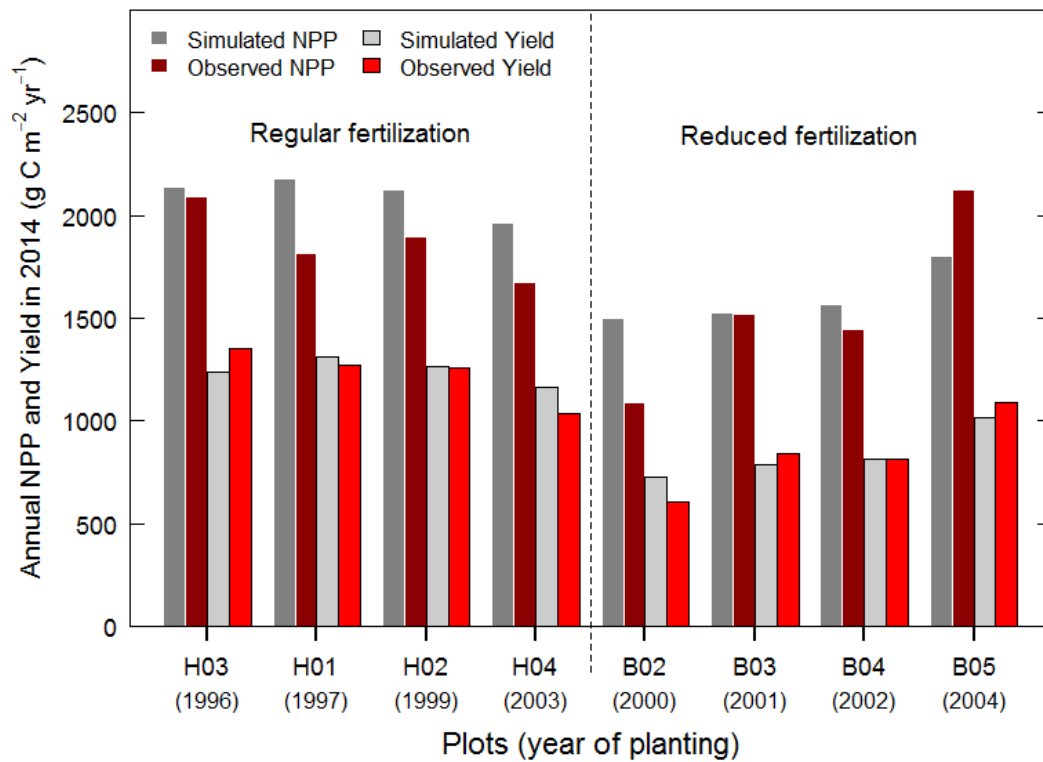
655



656

657 Fig. 9. Validation of LAI with 8 independent oil palm sites (sequence in plantation age) from
 658 the Harapan (regular fertilization) and Bukit Duabelas (reduced fertilization) regions: (a)
 659 shows the LAI development of each site simulated by the model since planting; (b) shows the
 660 comparison of field measured LAI in 2014 with model.

661



662

663 Fig. 10. Validation of yield and NPP with 8 independent oil palm sites from the Harapan (H)
 664 and Bukit Duabelas (B) regions with different fertilization treatments. Field data were
 665 collected in 2014.

666 **Appendix A**

667 Summary of main parameters

668 Table A1. Summary of new phenological parameters introduced for the phenology subroutine of CLM-Palm. The default values were determined by
 669 calibration and with reference to field observations and literatures on oil palm (Combres et al., 2013; Corley and Tinker, 2003; Hormaza et al., 2012; Legros
 670 et al., 2009).

Parameter	Default	Min	Max	Explanation (Unit)
<i>GDD_{init}</i>	0	0	1500	GDD needed from planting to the first phytomer initiation (°days). Initiation refers to the start of active accumulation of leaf C. A value 0 implies transplanting.
<i>GDD_{exp}</i>	1550	0	8000	GDD needed from leaf initiation to start of leaf expansion for each phytomer (pre-expansion) (°days)
<i>GDD_{L.mat}</i>	1250	500	1600	GDD needed from start of leaf expansion to leaf maturity for each phytomer (post-expansion) (°days)
<i>GDD_{F.fill}</i>	3800	3500	4200	GDD needed from start of leaf expansion to beginning of fruit-fill for each phytomer (°days)
<i>GDD_{F.mat}</i>	5200	4500	6500	GDD needed from start of leaf expansion to fruit maturity and harvest for each phytomer (°days)
<i>GDD_{L.sen}</i>	6000	5000	8000	GDD needed from start of leaf expansion to beginning of senescence for each phytomer (°days)
<i>GDD_{end}</i>	6650	5600	9000	GDD needed from start of leaf expansion to end of senescence for each phytomer (°days)
<i>GDD_{min}</i>	7500	6000	10000	GDD needed from planting to the beginning of first fruit-fill (°days)
<i>Age_{max}</i>	25	20	30	Maximum plantation age (productive period) from planting to final rotation /replanting (years)
<i>PLAI_{max}</i>	0.165	0.1	0.2	Maximum LAI of a single phytomer (m ² m ⁻²)
<i>mxlivenp</i>	40	30	50	Maximum number of expanded phytomers coexisting on a palm
<i>phyllochron</i>	130	100	160	Initial phyllochron (=plastochron): the period in heat unit between the initiations of two successive phytomers. The value increases to 1.5 times, i.e. 195, at 10-year old (°days)

671 Table A2. Summary of parameters involved in C and N allocation. The default values were determined by calibration and with reference to field
 672 measurements (Kotowska et al., 2015a).

Parameter	Defaults	Min	Max	Explanation (Unit)
$*f_{disp}$	0.3	0.1	1	Fraction of C and N allocated to the displayed leaf pool
$*transplant$	0.15	0	0.3	Initial total LAI assigned to existing expanded phytomers at transplanting. Value 0 implies planting as seeds.
f_{leaf}^i	0.15	0	1	Initial value of leaf allocation coefficient before the first fruit-fill
a_{root}^i	0.3	0	1	Initial value of root allocation coefficient before the first fruit-fill
a_{leaf}^f	0.28	0	1	Final value of leaf allocation coefficient after vegetative maturity
a_{root}^f	0.1	0	1	Final value of root allocation coefficient after vegetative maturity
F_{stem}^{live}	0.15	0	1	Fraction of new stem allocation that goes to live stem tissues, the rest to metabolically inactive stem tissues
d_{mat}	0.6	0.1	1	Factor to control the age when the leaf allocation ratio stabilizes at a_{leaf}^f according to Eq. 4
d_{alloc}^{leaf}	0.6	0	5	Factor to control the nonlinear function in Eq. 4. Values < 1 give a convex curve and those > 1 give a concave curve. Value 1 gives a linear function.
$*a$	0.2	0	1	Parameter a for fruit allocation coefficient A_{fruit} in Eq. 5
$*b$	0.02	0	1	Parameter b for fruit allocation coefficient A_{fruit} in Eq. 5
SLA	0.013	0.01	0.015	Specific leaf area ($m^2 g^{-1} C$)
F_{LNR}	0.1005	0.05	0.1	Fraction of leaf nitrogen in Rubisco enzyme. Used together with SLA to calculate V_{cmax25} ($g N Rubisco g^{-1} N$)

673 $*New$ parameters introduced for oil palm. Others are existing parameters in CLM but mostly are redefined or used in changed context.

674 Table A3. Other optical, morphological, and physiological parameters for oil palm.

Parameter	Value	Definition (Unit)	Comments
CN_{leaf}	33	Leaf carbon-to-nitrogen ratio (g C g ⁻¹ N)	By leaf C:N analysis
CN_{root}	42	Root carbon-to-nitrogen ratio (g C g ⁻¹ N)	Same as all other PFTs
CN_{livewd}	50	Live stem carbon-to-nitrogen ratio (g C g ⁻¹ N)	Same as all other PFTs
CN_{deadwd}	500	Dead stem carbon-to-nitrogen ratio (g C g ⁻¹ N)	Same as all other PFTs
CN_{lfit}	60	Leaf litter carbon-to-nitrogen ratio (g C g ⁻¹ N)	Same as other tree PFTs
CN_{fruit}	75	Fruit carbon-to-nitrogen ratio (g C g ⁻¹ N)	Higher than the value 50 for other crops because of high oil content in palm fruit
$r_{vis/nir}^{leaf}$	0.09/0.45	Leaf reflectance in the visible (VIS) or near-infrared (NIR) bands	Values adjusted in-between trees and crops
$r_{vis/nir}^{stem}$	0.16/ 0.39	Stem reflectance in the visible or near-infrared bands	Values adjusted in-between trees and crops
$\tau_{vis/nir}^{leaf}$	0.05/0.25	Leaf transmittance in the visible or near-infrared bands	Values adjusted in-between trees and crops
$\tau_{vis/nir}^{stem}$	0.001/ 0.001	Stem transmittance in the visible or near-infrared bands	Values adjusted in-between trees and crops
χ_L	-0.4	Leaf angle distribution index for radiative transfer (0 = random leaves; 1 = horizontal leaves; -1 = vertical leaves)	Estimated by field observation. In CLM, $-0.4 \leq \chi_L \leq 0.6$
<i>taper</i>	50	Ratio of stem height to radius-at-breast-height	Field observation. Used together with <i>stocking</i> and <i>dwood</i> to calculate canopy top and bottom heights.
<i>stocking</i>	150	Number of palms per hectare (stems ha ⁻²)	Field observation. Used to calculate stem area index (SAI) by: $SAI = 0.05 \times LAI \times stocking$.

<i>d_{wood}</i>	100000	Wood density (gC m ⁻³)	Similar as coconut palm (O. Roupsard, personal communication)
<i>R_{z0m}</i>	0.05	Ratio of momentum roughness length to canopy top height	T. June, personal communication
<i>R_d</i>	0.76	Ratio of displacement height to canopy top height	T. June, personal communication

- 676 Allen, K., Corre, M. D., Tjoa, A., and Veldkamp, E.: Soil nitrogen-cycling responses to
677 conversion of lowland forests to oil palm and rubber plantations in Sumatra, Indonesia,
678 PLoS ONE, 10(7), e0133325, doi:10.1371/journal.pone.0133325, 2015
- 679 Bonan, G. B., Levis, S., Kergoat, L., and Oleson, K. W.: Landscapes as patches of plant
680 functional types: An integrated concept for climate and ecosystem models, *Global*
681 *Biogeochemical Cycles*, 16 (2), 1021-1051, 2002.
- 682 Carlson, K. M., Curran, L. M., Asner, G. P., Pittman, A. M., Trigg, S. N., and Adeney, J. M.:
683 Carbon emissions from forest conversion by Kalimantan oil palm plantations, *Nature*
684 *Clim. Change*, 3(3), 283–287, doi:10.1038/nclimate1702, 2012.
- 685 Carrasco, L. R., Larrosa, C., Milner-Gulland, E. J., and Edwards, D. P.: A double-edged
686 sword for tropical forests, *Science*, 346(6205), 38-40, 2014.
- 687 Combres, J.-C., Pallas, B., Rouan, L., Mialet-Serra, I., Caliman, J.-P., Braconnier, S., Soulie,
688 J.-C., and Dingkuhn, M.: Simulation of inflorescence dynamics in oil palm and
689 estimation of environment-sensitive phenological phases: a model based analysis,
690 *Functional Plant Biology*, 40(3), 263-279, 2013.
- 691 Corley R. H. V. and Tinker, P. B. (Eds.): *The oil palm*, 4th edition, Blackwell Science,
692 Oxford, 2003.
- 693 Dee, D. P., Uppala, S. M., Simmons, A. J., Berrisford, P., Poli, P., Kobayashi, S., ... and
694 Vitart, F.: The ERA-Interim reanalysis: Configuration and performance of the data
695 assimilation system, *Quarterly Journal of the Royal Meteorological Society*, 137(656),
696 553-597, 2011.
- 697 Drewniak, B., Song, J., Prell, J., Kotamarthi, V. R., and Jacob, R.: Modeling agriculture in the
698 community land model, *Geoscientific Model Development*, 6(2), 495-515,
699 doi:10.5194/gmd-6-495-2013, 2013.
- 700 Euler, M.: *Oil palm expansion among Indonesian smallholders - adoption, welfare*
701 *implications and agronomic challenges*, Ph.D. thesis, University of Göttingen, Germany,
702 145 pp., 2015.
- 703 FAO. FAOSTAT Database, Food and Agriculture Organization of the United Nations, Rome,
704 Italy, available at: <http://faostat.fao.org/site/339/default.aspx> (last access: 17 June 2015),
705 2013.
- 706 Galloway, J. N., Dentener, F. J., Capone, D. G., Boyer, E. W., Howarth, R. W., Seitzinger, S.
707 P., ... and Vöösmary, C. J.: Nitrogen cycles: past, present, and future, *Biogeochemistry*,
708 70(2), 153-226, 2004.
- 709 Georgescu, M., Lobell, D. B., and Field, C. B.: Direct climate effects of perennial bioenergy
710 crops in the United States, *Proceedings of the National Academy of Sciences*, 108(11),
711 4307-4312, 2011.
- 712 Goh K. J.: Climatic requirements of the oil palm for high yields, in: *Managing oil palm for*
713 *high yields: agronomic principles*, Goh K.J. (Eds.), pp. 1–17, Malaysian Soc. Soil Sci.
714 and Param Agric. Surveys, Kuala Lumpur, 2000.
- 715 Guillaume, T., Damris, M., and Kuzyakov, Y.: Losses of soil carbon by converting tropical
716 forest to plantations: erosion and decomposition estimated by $\delta^{13}\text{C}$, *Global change*
717 *biology*, 21, 3548–3560, doi: 10.1111/gcb.12907, 2015.
- 718 Gunarso, P., Hartoyo, M. E., Agus, F., and Killeen, T. J.: *Oil Palm and Land Use Change in*
719 *Indonesia, Malaysia, and Papua New Guinea*. In: Killeen T, Goon J, editors. *Reports*
720 *from the Science Panel of the Second GHG Working Group of the Roundtable for*
721 *Sustainable Palm Oil (RSPO)*. Kuala Lumpur, 2013.
- 722 Hall é F., Oldeman, R. A. A. and Tomlinson, P. B.: *Tropical trees and forests. An*
723 *architectural analysis*. Springer-Verlag, Berlin, 441 pp., 1978.
- 724 Hijmans, R. J., Cameron, S. E., Parra, J. L., Jones, P. G., and Jarvis, A.: Very high resolution
725 interpolated climate surfaces for global land areas, *International journal of climatology*,
726 25(15), 1965-1978, 2005.

727 Hoffmann, M. P., Vera, A. C., Van Wijk, M. T., Giller, K. E., Oberthur, T., Donough, C., and
728 Whitbread, A. M.: Simulating potential growth and yield of oil palm (*Elaeis guineensis*)
729 with PALMSIM: Model description, evaluation and application, *Agricultural Systems*,
730 131, 1-10, 2014.

731 Hormaza, P., Fuquen, E. M., and Romero, H. M.: Phenology of the oil palm interspecific
732 hybrid *Elaeis oleifera* × *Elaeis guineensis*, *Scientia Agricola*, 69(4), 275-280, 2012.

733 Huth, N. I., Banabas, M., Nelson, P. N., and Webb, M.: Development of an oil palm cropping
734 systems model: lessons learned and future directions, *Environ. Modell. Softw.*, 62, 411–
735 419, doi:10.1016/j.envsoft.2014.06.021, 2014.

736 Jin, J. M. and Miller, N. L.: Regional simulations to quantify land use change and irrigation
737 impacts on hydroclimate in the California Central Valley, *Theoretical and Applied*
738 *Climatology*, 104, 429-442, 2011.

739 Koh, L. P. and Ghazoul, J.: Spatially explicit scenario analysis for reconciling agricultural
740 expansion, forest protection, and carbon conservation in Indonesia, *P. Natl. Acad. Sci.*
741 *USA*, 107, 11140–11144, doi: 10.1073/pnas.1000530107, 2010.

742 Kotowska, M. M., Leuschner, C., Triadiati T., Selis M., and Hertel, D.: Quantifying above-
743 and belowground biomass carbon loss with forest conversion in tropical lowlands of
744 Sumatra (Indonesia), *Global Change Biol.*, 21, 3620-3634, doi: 10.1111/gcb.12979,
745 2015a.

746 Kotowska, M. M., Leuschner, C., Triadiati, T., and Hertel, D.: Conversion of tropical lowland
747 forest lowers nutrient return with litterfall, and alters nutrient use efficiency and
748 seasonality of net primary productivity, *Oecologia*, submitted, 2015b.

749 Koven, C. D., Riley, W. J., Subin, Z. M., Tang, J. Y., Torn, M. S., Collins, W. D., Bonan, G.
750 B., Lawrence, D. M., and Swenson, S. C.: The effect of vertically resolved soil
751 biogeochemistry and alternate soil C and N models on C dynamics of CLM4,
752 *Biogeosciences*, 10(11), 7109-7131, doi:10.5194/bg-10-7109-2013, 2013.

753 Legros, S., Mialet-Serra, I., Caliman, J. P., Siregar, F. A., Clement-Vidal A., and Dingkuhn,
754 M.: Phenology and growth adjustments of oil palm (*Elaeis guineensis*) to photoperiod
755 and climate variability, *Annals of Botany* 104, 1171–1182. doi:10.1093/aob/mcp214,
756 2009.

757 Levis, S., Bonan, G., Kluzek, E., Thornton, P., Jones, A., Sacks, W., and Kucharik, C.:
758 Interactive crop management in the Community Earth System Model (CESM1):
759 Seasonal influences on land-atmosphere fluxes, *J. Climate*, 25, 4839-4859,
760 DOI:10.1175/JCLI-D-11-00446.1., 2012.

761 Luysaert, S., Schulze, E. D., Börner, A., Knohl, A., Hessenmöller, D., Law, B. E., Ciais, P.,
762 and Grace, J.: Old-growth forests as global carbon sinks, *Nature*, 455(7210), 213-215,
763 2008.

764 Miettinen, J., Shi, C. H. and Liew, S. C.: Deforestation rates in insular Southeast Asia
765 between 2000 and 2010, *Global Change Biology*, 17, 2261-2270, 2011.

766 Navarro, M. N. V., Jourdan, C., Sileye, T., Braconnier, S., Mialet-Serra, I., Saint-Andre, L., ...
767 and Rouspard, O.: Fruit development, not GPP, drives seasonal variation in NPP in a
768 tropical palm plantation, *Tree physiology*, 28(11), 1661-1674, 2008.

769 Oleson, K. W., Bonan, G. B., Levis, S., and Vertenstein, M.: Effects of land use change on
770 North American climate: impact of surface datasets and model biogeophysics, *Climate*
771 *Dynamics*, 23, 117-132, 2004.

772 Oleson, K., Lawrence, D., Bonan, G., Drewniak, B., Huang, M., Koven, C., Levis, S., Li, F.,
773 Riley, W., Subin, Z., Swenson, S., Thornton, P., Bozbiyik, A., Fisher, R., Heald, C.,
774 Kluzek, E., Lamarque, J.-F., Lawrence, P., Leung, L., Lipscomb, W., Muszala, S.,
775 Ricciuto, D., Sacks, W., Sun, Y., Tang, J., and Yang, Z.-L.: Technical description of
776 version 4.5 of the Community Land Model (CLM), National Center for Atmospheric
777 Research, Boulder, Colorado, USA, 420 pp., doi:10.5065/D6RR1W7M, 2013.

778 Tang, J. Y., Riley, W. J., Koven, C. D., and Subin, Z. M.: CLM4-BeTR, a generic
779 biogeochemical transport and reaction module for CLM4: model development,
780 evaluation, and application, *Geosci. Model Dev.*, 6, 127-140. doi:10.5194/gmd-6-127-
781 2013, 2013.

782 van Kraalingen, D. W. G., Breure, C. J., and Spitters, C. J. T.: Simulation of oil palm growth
783 and yield, *Agricultural and forest meteorology*, 46(3), 227-244, 1989.
784 Veldkamp, E., and Keller, M.: Nitrogen oxide emissions from a banana plantation in the
785 humid tropics, *Journal of Geophysical Research: Atmospheres* (1984–2012), 102(D13),
786 15889-15898, 1997.
787 White, M. A., Thornton, P. E., and Running, S. W.: A continental phenology model for
788 monitoring vegetation responses to interannual climatic variability, *Global Biogeochem.*
789 *Cycles*, 11, 217-234, 1997.
790